NeuroImage 49 (2010) 2774–2782

Contents lists available at ScienceDirect

NeuroImage

journal homepage: www.elsevier.com/locate/ynimg

Errors can be related to pre-stimulus differences in ERP topography and their concomitant sources

Juliane Britz [a,b,c,*], Christoph M. Michel [a,b,c,d]

[a] Department of Fundamental Neuroscience, Centre Médical Universitaire, University of Geneva, 1, Rue Michel Servet, CH-1211 Geneva, Switzerland
[b] Geneva Neuroscience Center, University of Geneva, Geneva, Switzerland
[c] EEG Brain Mapping Core, Center for Biomedical Imaging of Lausanne & Geneva (CIBM), Geneva, Switzerland
[d] Department of Neurology, University Hospital, Geneva, Switzerland

ARTICLE INFO

Article history:
Received 19 March 2009
Revised 9 October 2009
Accepted 12 October 2009
Available online 19 October 2009

Keywords:
Stroop task
ERP topography
Errors
High density ERPs
LORETA inverse solution
Pre-stimulus activity

ABSTRACT

Much of the variation in both neuronal and behavioral responses to stimuli can be explained by pre-stimulus fluctuations in brain activity. We hypothesized that also errors are the result of stochastic fluctuations in pre-stimulus activity and investigated the temporal dynamics of the scalp topography and their concomitant intracranial generators of stimulus- and response-locked high-density event-related potentials (ERPs) to errors and correct trials in a Stroop task. We found significant differences in ERP map topography and intracranial sources before the onset of the stimulus and after the initiation of the response but not as a function of stimulus-induced conflict. Before the stimulus, topographic differences were accompanied by differential activity in lateral frontal, parietal and temporal areas known to be involved in voluntary reorientation of attention and cognitive control. Differential post-response activity propagated both medially and laterally on a rostral–caudal axis of a network typically involved in performance monitoring. Analysis of the statistical properties of error occurrences revealed their stochasticity.

Introduction

Much of the variance of both neuronal and behavioral responses to stimuli can vary largely as a function of the pre-stimulus state of the brain. This pertains to spatial scales from single cells embedded in their local population to ERP map topographies and can be observed both in terms of longer-lasting aspects of pre-stimulus activity as well as the activity at the very moment of stimulus arrival. Pre-stimulus differences can affect both quantitative aspects of stimulus processing such as differences in reaction times and qualitative aspects such as detection or interpretation of stimuli. On the cellular level, variations in the magnitude of evoked responses have been related to both pre-stimulus fluctuations in membrane potentials (Azouz and Gray, 1999) and the overall state of the network a single neuron is embedded in (Arieli et al., 1996). On a global level, the ERP topography elicited by physically identical stimuli has been found to vary as a direct function of the immediate pre-stimulus topography (Kondakor et al., 1997; Kondakor et al., 1995; Lehmann et al., 1994). Quantitative behavioral aspects of stimulus processing, i.e. faster reaction times have been related to pre-stimulus power in the EEG gamma band both in monkeys (Womelsdorf et al., 2006) and humans (Gonzalez Andino et al., 2005). Likewise, slower reaction times have been consistently related to increased alpha power (Hanslmayr et al., 2007; Kranczioch et al., 2007; Romei et al., 2008a; Thut et al., 2006). Qualitative behavioral aspects of stimulus processing such as e.g. target detection and phosphene perception could be similarly related to pre-stimulus differences in alpha phase (Busch et al., 2009) and power (Hanslmayr et al., 2005; Rihs et al., 2007; Rihs et al., 2009; Thut et al., 2006; Romei et al., 2008a; Romei et al., 2008b). Other qualitative differences such as hemispheric lateralization in language processing (Mohr et al., 2005) or the perceptual interpretation of a bi-stable stimulus (Britz et al., 2009) could be related to the momentary state of the brain at stimulus onset as indexed by the EEG map topography. Thus, physically identical stimuli can undergo mutually exclusive fates as a function of momentary intrinsic brain dynamics before stimulus onset.

In the present study we took this assumption one step further and investigated whether error commission could also be attributed to differences in brain state in the time window immediately before stimulus arrival rather than to stimulus properties per se. Errors occur randomly, i.e. without a regular periodicity, and irrespective of physical stimulus properties. Errors are of course committed more likely under conditions of conflict or interference, i.e. when different response alternatives are mapped onto the same stimulus. It is important to note however, that errors are also committed in the absence of conflict or interference. Accordingly, differences before stimuli that are subsequently responded to correctly or erroneously should be the same irrespective of whether that stimulus induces a

* Corresponding author. Department of Fundamental Neuroscience, Centre Médical Universitaire, University of Geneva, 1, Rue Michel Servet, CH-1211 Geneva, Switzerland. Fax: +41 22 379 5728.
E-mail address: juliane.britz@unige.ch (J. Britz).

1053-8119/$ – see front matter © 2009 Elsevier Inc. All rights reserved.
doi:10.1016/j.neuroimage.2009.10.033

conflict or not. We hypothesized that pre-stimulus differences can lead to error commission rather than stimulus-induced conflict. Whether errors are committed because of failure in cognitive control or an incorrect stimulus–response mapping cannot be answered with the task used here.

We used a Stroop task because the mapping of multiple response alternatives onto the same stimulus induces conflict, which increases the likelihood of error commission. This enabled us to disentangle pre-stimulus and post-stimulus effects on errors. Effects of error commission as a consequence of pre-stimulus differences should manifest irrespective of conflict before stimulus onset. Error commission as a consequence of conflict should manifest after stimulus onset as a function of stimulus-induced conflict. We modified the Stroop task such that each response (i.e. each color) was mapped onto one finger. This was done to avoid contamination of the EEG by articulation-related muscle artifacts and to have distinct behavioral measures for each response alternative and clearly identifiable events for the computation of response-locked ERPs. We are aware that this induced a complex stimulus–response mapping which had to be held in working memory; note however, that this additional taxing on working memory affected both the conflict and non-conflict trials equally.

The consequences of error commission have been widely investigated. Errors elicit a large centrally distributed negativity (error-related negativity, ERN) which peaks at around 100 ms after response execution and whose generator has been localized in the anterior cingulate cortex (ACC) (Carter et al., 1998; Carter and van Veen, 2007; Debener et al., 2005; van Veen and Carter, 2002b). More recently, transient synchronous activity in the EEG theta band has been identified as the most likely generator of the ERN (Cavanagh et al., 2009; Luu et al., 2004; Trujillo and Allen, 2007). Theta power, i.e. coherent phase locking in the theta frequency band, has been found to decrease in trials preceding errors and to increase immediately after the commission of an error.

The erroneously treated stimuli themselves on the other hand have received surprisingly little attention and are usually discarded as −errors. Previous studies have found larger positive deflections (error-preceding positivity, EPP) at two central electrodes in the first 100 ms after the response in trials preceding an error than a correct response (Hajcak et al., 2005; Ridderinkhof et al., 2003). This has been interpreted as fluctuations in the efficiency of action monitoring without further investigations of concomitant sources. If errors are indeed foreshadowed by decreased levels of action monitoring, these differences should manifest beyond the first 100 ms after response execution. If such transient failures of action monitoring are the cause for errors in a subsequent trial, they should manifest in time-locked differences in action monitoring and cognitive control, and this should still be observed immediately before stimulus onset in a subsequent trial.

We hypothesized that errors can be related to stochastic fluctuations in pre-stimulus differences in brain state and disentangled the time course of both stimulus- and response-locked brain activity in a Stroop task (MacLeod, 1991) by means of Electrical Neuroimaging (Michel et al., 2004; Murray et al., 2008). We investigated differences in ERP scalp topographies as a function of error commission. Since different topographies have necessarily different intracranial generators, we also estimated differences in their concomitant sources. Like all EEG/MEG source localization methods, the distributed inverse solutions are non-unique and depend on the implemented constraints and the regularization parameters. However, numerous experimental and clinical studies have shown that the constraints introduced in the distributed linear inverse solutions lead to reasonable results. Such studies included direct comparison with intracranial recordings and electrocortical stimulation (Fuchs et al., 1999; Lantz et al., 1996; Michel et al., 1999a; Zumsteg et al., 2006), with fMRI (Groening et al., 2009; Schulz et al., 2008; Vulliemoz et al., 2009) and with post-surgical outcome (Michel et al., 2004; Sperli et al., 2006).

In the framework of the current hypothesis, namely that errors are the consequence of pre-stimulus differences in brain activity rather than the mere presence of conflict, the distinction between errors and correct responses should manifest before the onset of the stimulus and after the initiation of the response irrespective of the stimulus-induced conflict.

Methods

Subjects

Eleven subjects (five female) participated in exchange for monetary compensation. All were right-handed (Oldfield, 1971), native speakers of French and had normal or corrected-to-normal visual acuity and none had any current or prior neurological or psychiatric impairments. Mean age of participants was 27.63 years (range 20–31 years). Prior to participation, subjects provided written informed consent that had been approved by the Medical Ethics Committee of the University Hospital of Geneva in compliance with the Declaration of Helsinki.

Stimuli and procedure

Stimuli were four French color words for red, yellow, green and blue ("rouge", "jaune" , "vert", "bleu") each written in red, blue, green and yellow, respectively. In congruent trials, the ink color and the color word referred to the same, and in incongruent trials they referred to different colors. Stimuli were presented in the center of a CRT screen for 200 ms and subtended ~2.5° of horizontal visual angle. Subjects were seated about 100 cm from the screen and were instructed to indicate the color of the ink by using their right hand (index = red, middle = yellow, ring = green, pinkie = blue). This was done to avoid contamination of the EEG by muscular artifacts associated with the pronunciation of the color. Prior to the EEG experiment, a behavioral training session familiarized subjects with the procedure and allowed them to practice the association of the ink colors with the corresponding fingers.

Each trial started with the presentation of a fixation cross whose duration was randomly varied between 500 and 2000 ms; this was done to prevent subjects from anticipating the precise onset of the stimulus presentation. The stimulus was presented for 200 ms followed by a fixation cross which remained on the screen until the response (max. 2000 ms). After the response, a feedback was given to the subjects (200 ms), then the fixation cross reappeared for 500 ms and it turned green for 1000 ms to indicate the time period when subjects were allowed to blink (see Fig. 1). Subjects were instructed to

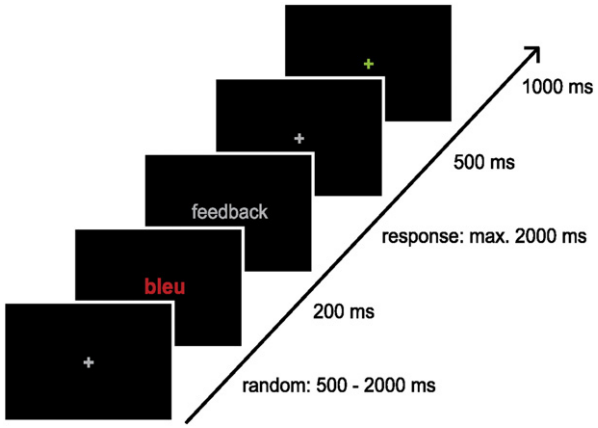

Fig. 1. Experimental procedure. After a random inter-trial interval, the stimulus was displayed for 200 ms, and response feedback was given. The green cross indicated when subjects were allowed to blink.

perform as fast and accurately as possible and to try to refrain from blinking until the fixation cross had turned green.

Equal numbers of congruent and incongruent trials were used, and subjects performed a total of 600 trials which were equally distributed over four blocks, each of which lasted about 11 min.

Analysis of behavioral data

We computed average reaction times (RTs) for each subject for the Congruent and Incongruent Error and Correct conditions, respectively. We assessed error rates for the Congruent and Incongruent conditions separately for each response finger. We then further assessed the statistical properties of the occurrence of errors by means of their distribution and autocorrelation function (Britz et al., 2009). This was done to assess the stochasticity and hence the irregularity of the assumed pre-stimulus fluctuations in cognitive control. In order to evaluate the autocorrelation function for subsequent errors, we computed for each subject the correlation of the number of intervening trials between subsequent errors for each trial n with that in trial $n+m$ for $m=1$–10; this indicates how well the next 10 errors could be predicted from an error in trial n. In order to test the distribution of the duration of the inter-error lags, we computed Maximum Likelihood Estimates from the cumulative probability distribution both of the scale and shape parameters (α and β) of the gamma distribution and mean and standard deviation (μ and σ) of the lognormal distribution. A Kolmogorov–Smirnov test was used to test for each of these distributions.

EEG acquisition and data reduction

The EEG was recorded from 256 AgCl carbon-fiber coated electrodes using a Hydrocel Geodesic Sensor Net®. The vertex was used as the recording reference, and EEG was continuously digitized at 1 kHz and band-pass filtered between 0.1 and 100 Hz; impedances were kept below 30 kΩ; off-line, the EEG was re-calculated to the common average reference. The channels located on the cheeks and below the Nz–Iz equator were omitted and the remaining 204 channels were submitted to further analysis.

Before segmenting the EEG data into epochs, the ongoing EEG was band-pass filtered between 1 and 30 Hz. A 2nd order Butterworth filter with a −12 db/octave roll-off was used. The filter was computed linearly with two passes (one forward and one backward), eliminating the phase shift, and with poles calculated each time to the desired cut-off frequency. To investigate approximately similar time periods before stimulus onset and response onset, we used different time periods to examine these effects. Pre-stimulus effects can be clearly linked to the physical onset of the stimulus. Responses however are initiated in the motor cortex approximately 100 ms before the execution of the button press; estimated transduction time between motor cortex and finger muscle in the monkey is about 70 ms (Thorpe and Fabre-Thorpe, 2001). For stimulus-locked effects we will always refer to stimulus onset, for response-locked effects, we will make a distinction between assumed response initiation (in motor cortex, approximately 100 ms before the button press) and response execution (the registered button press). Stimulus-related evoked potentials were computed for both the Correct and Error conditions over an epoch of 600 ms encompassing a pre-stimulus window of 100 ms. Response-related evoked potentials were computed over an epoch of 600 ms with a pre-response window of 200 ms; no baseline correction was applied to the data to avoid averaging out pre-stimulus differences that we believe are of importance (Britz et al., 2009).

The epochs were visually inspected for oculomotor and other artifacts in addition to an automated threshold rejection criterion of 75 μV. Channels exhibiting substantial noise were interpolated using a 3D spherical spline interpolation procedure (Perrin et al., 1989); on average, 1.25 channels were interpolated per subject.

Analysis of stimulus- and response-locked ERPs

We compared the stimulus- and response-locked ERPs elicited in both correct and error trials by using both a global and a local measure.

First, we applied a spatio-temporal segmentation procedure (Michel et al., 2004; Michel et al., 1999b) to identify the successive stable map topographies of the grand average correct and error conditions for both the stimulus- and response-locked ERPs. This determined whether the different conditions evoke the same scalp potential fields across time or not (Arzy et al., 2007; Ducommun et al., 2002; Michel et al., 2001; Murray et al., 2008; Thierry et al., 2007). This approach follows the notion that the ERP map topography does not vary randomly across time but that it remains stable for successive processing states with rapid transitions between states. A spatial Atomize-Agglomerate Hierarchical (AAHC) cluster analysis (Tibshirani and Walther, 2005) identified the most dominant clusters (or template maps) that best describe the scalp topographies. The optimal number of template maps was determined by means of a modified Krzanowski–Lai criterion (Krzanowski and Lai, 1988). Map durations of less than 10 ms were considered physiologically implausible and we set a temporal constraint criterion for minimum map duration to be >10 ms.

Next, we determined whether the map topographies identified in the grand average evoked potential could be identified in the individual subjects. For each subject, we computed a strength-independent spatial correlation between the series of template maps identified in the Grand Average with the individual data. It was then statistically assessed how frequently each map was identified in each subject and how much of the Global Variance it explained.

In order to compare our results with conventional ERP analysis approaches, we also assessed amplitude differences between the error and correct trials in both stimulus- and response-locked ERPs by performing multiple t-tests for each electrode and time point to determine time periods of significant differences; the significance level was set to be $p=0.01$ with a minimum duration of 10 ms and without further correction for multiple comparisons. We conducted an ANOVA with the factors Congruence and Accuracy to investigate their common influence on error commission.

In order to assess whether topographies differed as a function of stimulus-induced conflict or were merely obtained before stimulus arrival, we applied a spatial–temporal segmentation procedure to all four stimulus conditions (Congruent Correct, Incongruent Correct, Congruent Error, Incongruent Error). Incongruent conditions refer to stimulus-induced conflict and Congruent conditions refer to the absence of stimulus-induced conflict.

Finally, we assessed the issue whether topographic differences between error and correct trials for the stimulus-locked ERPs could have arisen from different numbers of trials submitted to the average. For each subject, we drew two random subsamples from the correct trials with the same number as the error trials. We then compared the topographies of the Grand Averages containing all samples and containing only the two subsamples.

Analysis of evoked potential sources

We used a LORETA linear inverse solution (Michel et al., 2004; Pascual-Marqui et al., 1994) to estimate the intracranial current distribution at each time point for each condition and each subject. Since the inverse problem is ill-posed, we used conservative statistical analyses to investigate differences between the source estimations between the two conditions, which eliminates all spurious sources of activity. The current distribution was calculated in a discrete grid of 3005 solution points that was regularly distributed within the gray matter of the cerebral cortex and limbic structures of the average brain provided by the Montreal Neurological Institute (MNI 152 average brain). After applying a homogeneous transformation

operation to the volume that rendered it to the best fitting sphere (SMAC model; Spinelli et al., 2000), a 3-shell spherical head model was used to calculate the lead field for the 204 electrodes and the inverse solution based on the LORETA constraint. The solution space was then spatially smoothed by subdividing the 3005 solution points into 80 anatomical regions of interest (ROI) that were defined according to the macroscopic anatomical parcellation of the MNI template according to the Automated Anatomical Labeling (AAL) map (Tzourio-Mazoyer et al., 2002) available from the MRIcro software (Rorden and Brett, 2000). Similar to the statistical parametric mapping used in fMRI analysis, we computed time-point wise paired *t*-tests (two-tailed) between experimental conditions for the 80 regions of interest. *p*-values were adjusted using a Bonferroni-correction for multiple testing ($n=79$, $p=0.0063$).

Results

Behavioral results

Reaction times and accuracies are summarized in Figs. 2a and b.

A 2×2 ANOVA with the factors Congruence (Congruent, Incongruent) and Accuracy (Correct, Error) revealed a main effect of Congruence ($F(1,10)=62.12$; $p<0.01$), but not of Accuracy ($F<1$). The interaction of Congruence and Accuracy was not significant ($F(1,10)=1.05$, $p=0.3$). Mean reaction times in the Congruent condition were 591 ms and 582 ms for the Correct and Error conditions, respectively, and mean reaction times in the Incongruent condition were 670 ms and 688 ms for the Correct and Error conditions, respectively. Error rates in the Congruent condition were 5.17% and in the Incongruent condition 7.91%; this difference was significant ($t=0.017$). The 4×2 ANOVA on the numbers of errors with the factors Finger (4 levels) and Condition (Congruent, Incongruent) revealed a main effect of Finger ($F(3,10)=5.03$, $p=0.009$) and Condition ($F(1.10)=4.64$, $p=0.03$), but no interaction between the two factors ($F(1,10)=1.8$, $p=0.15$).

Errors occurred on average on every 16.01th (Median=11, SD=14.15) trial; the autocorrelation function for the inter-error lags between an error in trial n and a subsequent error in trials $n+m$ is plotted in Fig. 3a. For $m=1$–10, no correlations were obtained between subsequent inter-error lags. Figs. 3b and c show the probability density and the cumulative probability functions, respectively. A Kolmogorov–Smirnov test revealed that the inter-error lags followed a gamma ($\alpha=1.59$, $\beta=10.067$, $p<0.01$) and a lognormal ($\mu=2.4278$, $\sigma=0.8564$, $p<0.001$) function.

Evoked potentials

The analysis steps are laid out in detail in the Methods section. We first report the results of the stimulus-locked and then of the response-locked ERPs.

Stimulus-locked ERPs

The spatio-temporal segmentation of the 3 samples of correct stimulus-locked ERPs revealed 8 template maps which explained 90.0% of the variance (see Supplementary Fig. 1). Topographies did not differ between the three conditions, and we used the sample containing all trials for all subsequent analyses.

The spatio-temporal segmentation procedure identified 9 template potential maps which explained 91.94% of Global Variance in both conditions; the results are depicted in the top panel in Fig. 4a. Significant differences in map occurrence were obtained only before, but not after the onset of the stimulus. A double dissociation of map presence was found before the onset of the stimulus: Map 1 occurred significantly more often before subjects committed an error ($t=2.75$, $p=0.02$), and Map 2 occurred significantly more often when subjects responded correctly ($t=-2.75$, $p=0.02$). No post-stimulus differences in map presence were found. The spatio-temporal segmentation of all four stimulus conditions identified 10 template maps which explained 91.89% of the variance. No post-stimulus differences reached significance. Visual inspection might suggest a difference in field strength between error and correct conditions at around 230 ms after stimulus onset. In the global spatial analysis across all electrodes, this difference failed to reach significance. ERP waveforms from seven exemplar electrode sites are depicted in the top panel of Fig. 5a. Conventional waveform analyses at each electrode revealed amplitude differences between the error and correct conditions in a time window ranging from 200 to 260 ms after stimulus onset in an occipital and a fronto-central cluster of electrodes (bottom panel of Fig. 5a). Over the occipital electrode cluster, amplitudes were larger in the Correct than the Error condition with a polarity inversion over the fronto-central cluster. Neither this cluster of amplitude difference nor the subsequent one in the time window 380–500 ms was accompanied by any differences in map topography or intracranial generators. Finally, the ANOVA with the factors Congruence and Accuracy revealed no significant interaction between Congruence and Accuracy.

Response-locked ERPs

The top panel of Fig. 4b shows the results of the spatio-temporal segmentation procedure; it identified 9 template maps which explained 85.43% of the Global Variance. Unlike the stimulus-locked ERPs, which elicited topographic differences only before stimulus onset, response-locked ERPs only differed after the initiation of the response. Scalp topographies were identical in the 100 ms before the initiation of the response (−200 to −100 ms) and differed between −100 and 160 ms around the execution of the button press.

Unlike for the stimulus-locked ERPs, conventional waveform analyses corroborate the findings of the topographic analyses. The top panel of Fig. 5a shows ERP waveforms from seven exemplar electrode sites. The amplitude differences in the time window −200–400 ms are accompanied the differences in topography. Erroneous

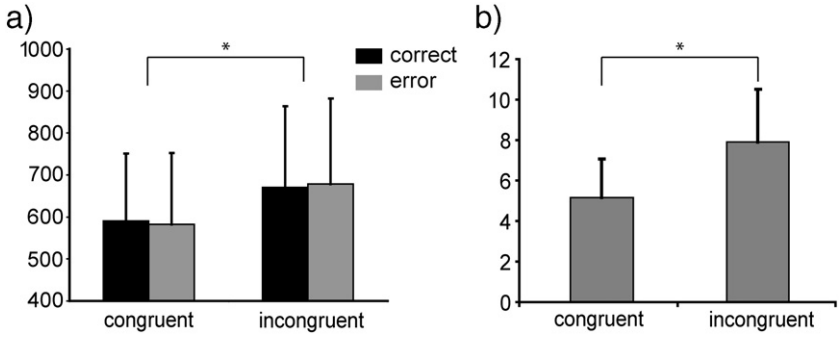

Fig. 2. (a) Mean reaction times (in ms) and b) error rates (in %), error bars denote standard deviations. Reaction times were significantly faster for congruent than incongruent trials, irrespective of accuracy, and subjects committed more errors in the incongruent than the congruent condition.

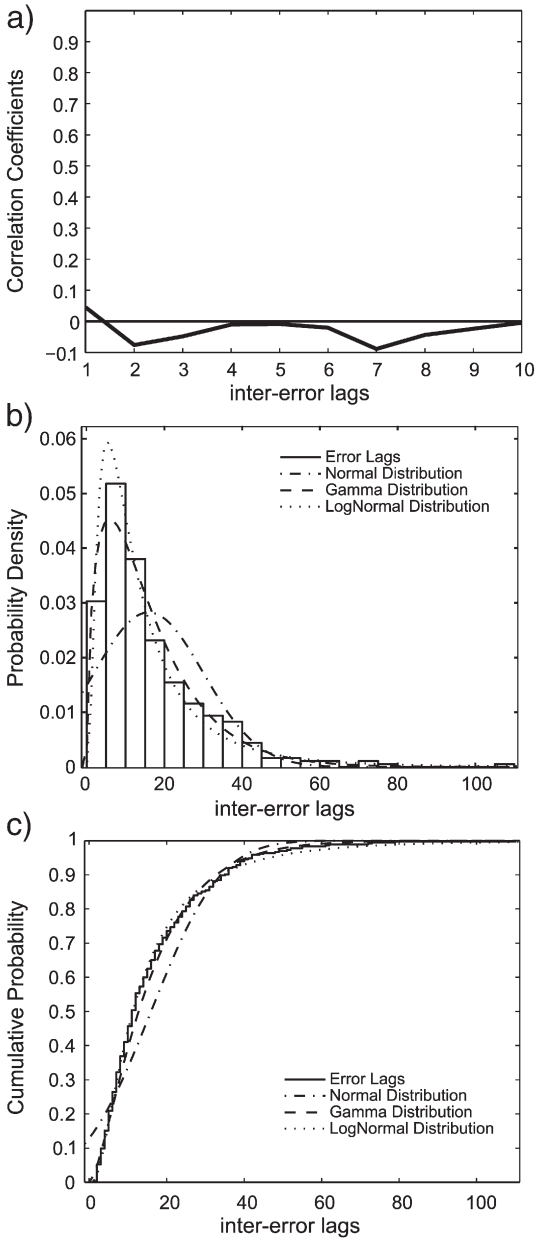

Fig. 3. Statistical properties of the errors. (a) Autocorrelation function of errors. Correlations between the probability of committing an error in a current trial with that in the next up to 10 trials; correlation coefficients are plotted on the *y* axis. (b) Histogram of the probability density function of the inter-error lags. The dashed–dotted line displays the fitted gamma probability distribution, the dashed line displays the fitted gamma distribution, and the dotted line displays the fitted normal distribution. (c) The cumulative probability distribution for the inter-error lags. The dashed–dotted line displays the fitted gamma probability distribution, the dashed line displays the fitted gamma distribution, and the dotted line displays the fitted normal distribution.

responses elicited a strong negative-going wave peaking at ~100 ms after response execution which has the typical time course and morphology of the error-related negativity (ERN) and which is followed by a positive wave (error-positivity, P_E). The bottom panel of Fig. 5b displays the time course of amplitude differences along with their scalp locations. Significant amplitude differences were obtained in the time windows −73–137 ms around the response. ERPs were significantly more negative to errors than correct responses over a large cluster of central electrodes. It was followed by a second cluster of significant amplitude differences in the window 229–400 ms at a similar scalp location; in this time window, ERPs were more positive in the error than the correct trials.

Results of ERP sources

Stimulus-locked source differences

The bottom panel of Fig. 4a displays the time course of statistical differences between Error and Correct conditions for the stimulus-locked differences in current source distribution. Significant differences ($p<0.05$, corrected for multiple comparisons, minimum duration = 10 ms) were found virtually only in the 100 ms preceding the stimulus onset. Decreased activation in the Error conditions were found in bilateral lateral and medial frontal and medial parietal areas encompassing the bilateral precentral gyri, bilateral superior frontal gyri, bilateral middle frontal gyri, bilateral superior medial frontal gyri, right precuneus, right supramarginal gyrus. Moreover, significant decreases in activity were found in primary visual areas (right superior occipital lobe, right cuneus). In some areas, these differences persisted beyond stimulus onset; importantly, we found no area that shows solely post-stimulus differences, i.e. all areas that show post-stimulus differences also show pre-stimulus differences.

Response-locked source differences

Unlike for the stimuli, significant differences for the response-related activity were found in two time windows only after its initiation. The bottom panel of Fig. 4b displays the time course of statistical differences between error and correct trials for the response-locked source distribution.

We identified two consecutive time windows of significant differences: activity spread in an extended network along a rostral–caudal axis both medially and laterally from frontal to parietal areas. In the first time window which coincides with that of the ERN surface differences (52–112 ms after response execution), significant differences with increased activity in the Error condition were obtained in a network of medial and lateral frontal areas. Medially, it encompassed bilateral anterior cingulate gyri as well as superior medial frontal gyri. Laterally, it encompassed bilateral precentral, superior and middle frontal gyri, bilateral supplementary motor area. The second window of significant differences (220–300 ms after the response) corresponds to that of the P_E; during this time period, significant differences were found in more caudal areas which encompassed medially the middle cingulate gyrus as well as bilateral paracentral lobules, and laterally, it encompassed laterally bilateral supplementary motor areas as well as the superior parietal gyri.

Discussion

We used Electrical Neuroimaging to delineate the time course of both stimulus- and response-locked differences in brain activity for errors and correct trials in a Stroop task. The primary finding of the present study is that erroneous responses in a high-conflict task can be related to differential pre-stimulus activity both in terms of global topography as well as the distribution of the active sources in the brain.

ERP scalp topographies differed only before the onset of erroneously vs. correctly treated stimuli and never as a consequence of stimulus-induced conflict which supports our hypothesis that errors can be related to pre-stimulus differences in brain activity. This finding is also in line with several other studies which have shown that qualitative aspects of stimulus processing such as target detection and stimulus perception can be related to pre-stimulus differences in another property of the EEG, namely phase (Busch et al., 2009) and spectral power in the alpha band (Hanslmayr et al., 2007; Rihs et al., 2007; Rihs et al., 2009; Romei et al., 2008a; Romei et al., 2008b; Thut et al., 2006).

Since different scalp topographies always indicate different neuronal generators, we also estimated their differential concomitant generators and found differences in the dorsal fronto-parietal

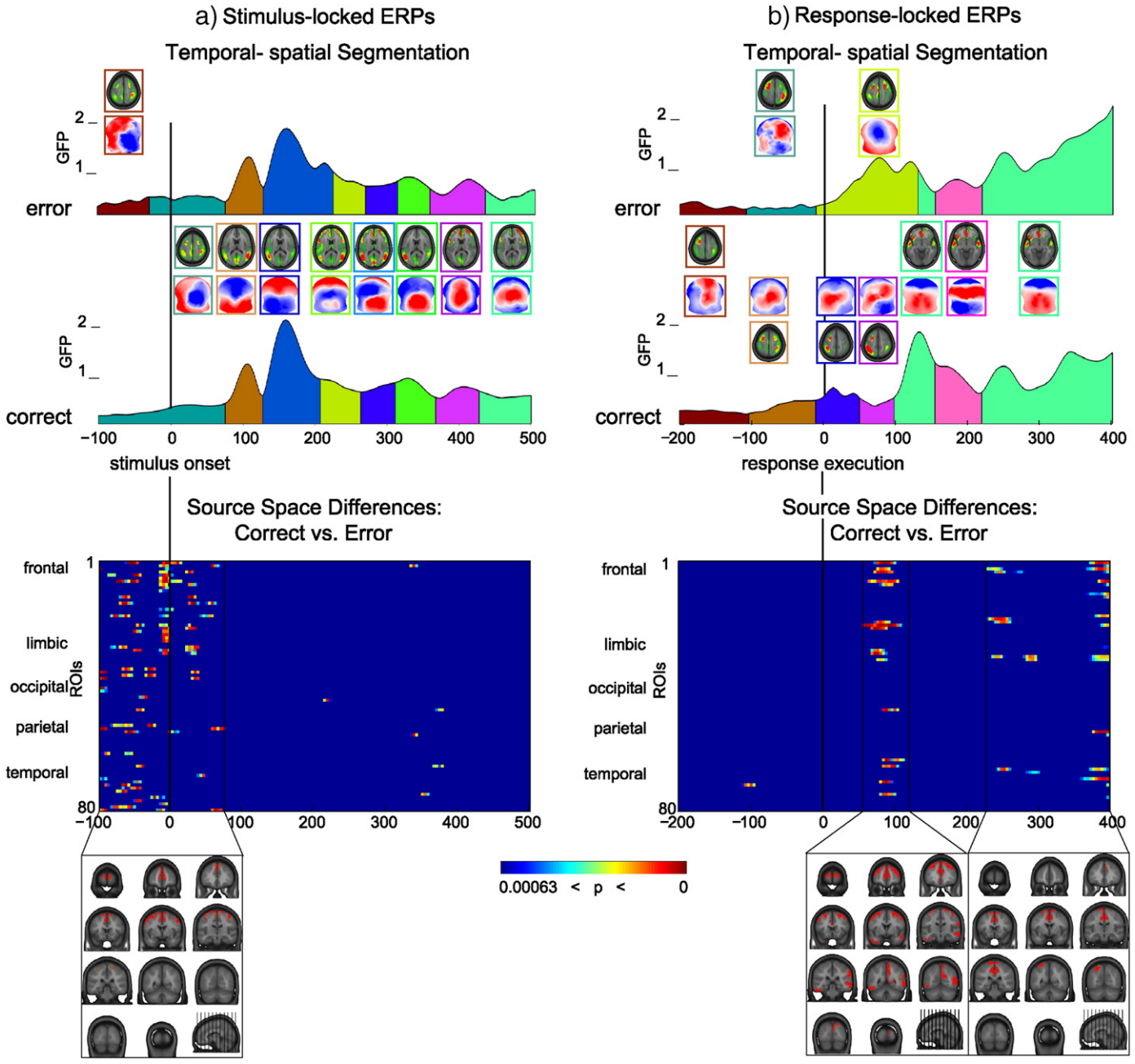

Fig. 4. Temporal spatial segmentation and source space differences. (a) Stimulus locked ERPs. The temporal spatial segmentation procedure yielded 9 template maps which are displayed in the top panel for the error and correct conditions. Maps are displayed with the left hemifield on the left and the nose on top as a function of time for the time window −100–500 ms. Stimulus onset is indicated by a black vertical bar. Significant differences in map topography were found only before, but not after stimulus onset. Maxima of source estimations are given for each template map. The same color code is used for corresponding maps and source images. Source space differences are displayed in the bottom panel for 80 anatomically defined regions of interest (ROIs). Significant differences were found primarily before the onset of the stimulus in frontal and parietal as well as temporal and limbic regions depicted below. (b) Response-locked ERPs. The temporal spatial segmentation procedure yielded 9 template maps which are displayed in the top panel for the error and correct conditions. Maps are displayed wit the left hemifield on the left and the nose on top as a function of time for the time window −200–400 ms. Response execution is indicated by a black vertical bar. Significant differences in map topography were obtained only after the initiation of the response. Maxima of source estimations are given for each template map. The same color code is used for corresponding maps and source images. Source images for maps common to both conditions are depicted above the map images, and source images idiosyncratic to the correct condition are depicted below the map images. Source space differences are displayed in the bottom panel for 80 anatomically defined ROIs. Significant differences were found in two time windows after the execution of the response both medially and laterally on a rostral–caudal axis. They are depicted below.

network known to be involved in reorientation of attention (Corbetta, 1998; Corbetta et al., 2008) and the more ventral network implicated in cognitive control (Brass et al., 2005a; Brass et al., 2005b) as well as in primary visual areas. Source estimations are by nature non-unique and depend on the implemented constraints and the regularization parameters and are not a direct measurement of neuronal activity. We report differences between conditions identified by applying conservative statistical testing to source estimations, which reduces the contribution of spurious sources. The direct source estimations depicted in Fig. 4 are for illustrative purposes only.

No such differences were found for the scalp potentials and their generators after the onset of the stimuli. The areas identified here are virtually the same that have been associated with attentional lapses indexed by increased reaction times (Weissman et al., 2006). We took the notion of attentional lapses one step beyond longer reaction times, namely the commission of an error. We find a very similar pattern of

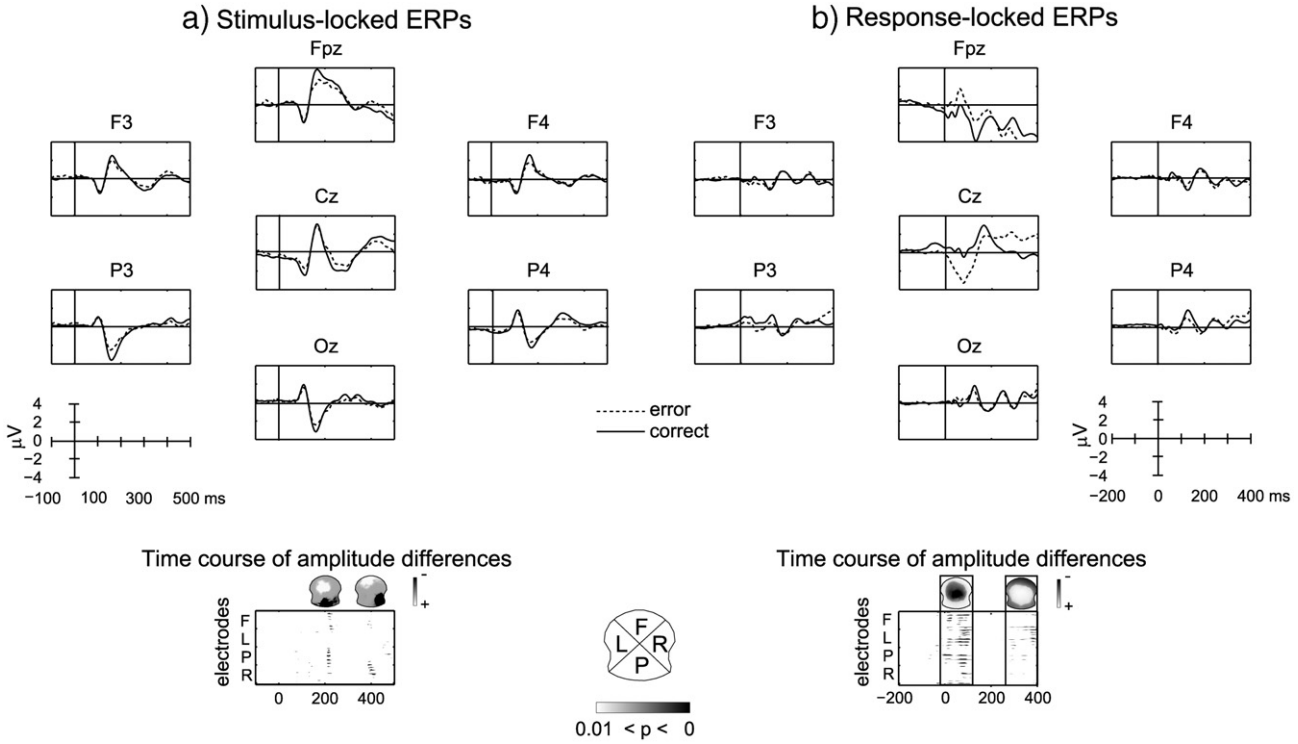

Fig. 5. Stimulus-locked and response-locked Grand Average ERP waveforms. a) Stimulus-locked ERPs. The top panel shows Grand Average ERPs for the error and correct conditions at 7 exemplar electrode sites in the time window −100–500 ms. ERPs to errors are displayed in a dotted line and correct responses in a solid line; positive potentials are plotted up. Significant differences between the error and correct conditions were found in two brief time windows around 200 ms and 400 ms. Their time course and location are shown in the bottom panel. They were not accompanied by source space differences. b) Response-locked ERPs. The top panel shows Grand Average ERPs for the error and correct conditions from 7 exemplar electrode sites in the time window −200–400 ms. ERPs to errors are displayed in a dotted line and correct responses in a solid line; positive potentials are plotted up. Significant differences between the error and correct conditions were found in two time windows after response execution. Their time course and location are shown in the bottom panel. These amplitudes were accompanied by source space differences depicted in Fig. 4b.

results as Weissman et al., namely that reduced activations in areas involved in the focus of attention lead to a decrease in top-down bias on sensory areas. This might be a consequence of a brief breakdown in action monitoring in the preceding trial which persists until immediately before stimulus onset in the current trial (Hajcak et al., 2005; Ridderinkhof et al., 2003).

The waveform analyses revealed amplitude differences between error and correct trials in two time windows around 200 ms and 400 ms after stimulus onset. They were not accompanied by global differences in topography nor in current density. There is thus no direct evidence for significant differences in configuration or strengths of the sources activated in these post-stimulus time periods. Nevertheless, the waveform analysis indicates that stimuli that were incorrectly responded to were also processed slightly differently.

This is indicative of differences in the strength of the same underlying sources; however, these differences source strength did not reach statistical significance.

Even though subjects committed more errors in the Incongruent than the Congruent condition, i.e. under conditions of conflict, this did not manifest in an interaction between the factors Congruence and Accuracy in the waveform analysis. In other words, the effects of stimulus-induced conflict did not differ between errors and correct responses. This unexpected result is most likely caused by the complex stimulus–response mapping employed in our adaptation of the Stroop task which has led to an unusually high error rate in the Congruent condition.

The results from the combined topographic and waveform analyses on the stimulus-locked ERPs reveal that errors can be related to pre-stimulus source differences in frontal and parietal areas. These pre-stimulus differences in ERP topography, followed by post-stimulus amplitude differences lead to errors independent of the level of stimulus congruency.

We investigated the stochasticity of error occurrences by means of the autocorrelation function and the distribution of the inter-error-lags. The autocorrelation analysis shows that from an error in any given trial, the next up to 10 errors can not be predicted, and the inter-error lags follow a gamma- and a lognormal distribution; from this we can not conclude that errors follow a regular pattern but rather occurred sporadically and without a clear periodicity. We find support for our hypothesis that errors are a function of stochastically varying brain activity irrespective of stimulus-induced conflict.

One could argue that the different numbers of trials in the error and correct conditions and therefore a different SNR might have biased the effects. We could rule out that differences in SNR yield different topographies and thus different sources by comparing the topographies elicited by the entire sample of correct trials and two random subsamples that had the same number of trials as the error condition. We can thus rule out that one of the major effects of our experiment, namely significant differences in current source before stimulus onset is due to differences in noise between the two conditions.

Scalp ERPs and their concomitant intracranial sources only differed *after* the initiation of a response. The transduction time between the initiation of the motor command in motor cortex and the movement of the finger muscle has been estimated to be about 70 ms in the monkey (Thorpe and Fabre-Thorpe, 2001); given the longer pathway, it is probably about 100 ms in humans. Thus, the identical topography in the time window −200 to −100 ms before the registered button press indicates that correct and erroneous responses are not initiated differently in motor cortex. However, after the motor command has been sent to the finger muscle, differences in topography can be identified between correct and erroneous responses. Thus, correct and erroneous responses appear not to be initiated, but acknowledged differently.

Response-locked scalp ERPs differed between correct and error trials in two time windows after the execution of the response. Their concomitant sources differed in two time windows. Sources for the ERN were not only found in the ACC, but also in more widespread medial and lateral frontal areas. The ACC source is concordant with previous ERP source localization and fMRI studies (Debener et al., 2005; Herrmann et al., 2004; van Veen and Carter, 2002a, b). The sources for the P_E were localized in the middle and anterior cingulate cortex, bilateral superior frontal gyri, as well as the paracentral lobule. These sources are more widespread than what has been identified in previous studies which have identified a single source in ACC. These studies have used either the peak maximum of the grand average difference wave between error and correct conditions (van Veen and Carter, 2002b) or the grand average independent component map of the ERN (Debener et al., 2005). The time-point wise statistical comparison in the inverse space we used here does not estimate a single dipole source, but it takes into account the temporal dynamics of the inter-individual variability in the two conditions.

In our adaptation of the Stroop task, a rather complex mapping between stimuli and responses had to be maintained in working memory, which might have contributed to the rather high error rates observed in the Congruent condition. This might explain the rather widespread activity differences obtained in left frontal areas involved in working memory maintenance. Note however, that this potentially additional source for errors has the same effects before the arrival of the stimulus and does consequently not differ between stimuli that subsequently induce conflict or not. We found differences in errors for the different response fingers, but these did not differ between the Congruent and Incongruent conditions. This shows that the output channel, i.e. the response finger is a major source of error commission and not so much the conflict between stimulus and response.

Our results are more compatible with the view that errors are the consequence of momentary stochastic changes in brain activity in areas involved in successful maintenance of task effort. Taken together, we can relate errors to pre-stimulus differences in ERP topography and their concomitant sources, but not stimulus-induced conflict. The complex stimulus–response mapping employed in the present study might have been the most probable source of error commission, since it differed between the different response fingers, but not differentially so between the two conditions. Moreover, correct and erroneous responses are also not initiated differently, and brain activity differs only after their commission.

Acknowledgments

This work was supported by the Swiss National Science Foundation (3200-111783) to C.M.M.

The Cartool software (http://brainmapping.unige.ch/Cartool.htm) has been programmed by Denis Brunet from the Functional Brain Mapping Laboratory, Geneva, Switzerland, and is supported by the Center for Biomedical Imaging of Geneva and Lausanne.

Appendix A. Supplementary data

Supplementary data associated with this article can be found, in the online version, at doi:10.1016/j.neuroimage.2009.10.033.

References

Arieli, A., Sterkin, A., Grinvald, A., Aertsen, A., 1996. Dynamics of ongoing activity: explanation of the large variability in evoked cortical responses. Science 273, 1868–1871.

Arzy, S., Mohr, C., Michel, C.M., Blanke, O., 2007. Duration and not strength of activation in temporo-parietal cortex positively correlates with schizotypy. Neuroimage 35, 326–333.

Azouz, R., Gray, C.M., 1999. Cellular mechanisms contributing to response variability of cortical neurons in vivo. J. Neurosci. 19, 2209–2223.

Brass, M., Derrfuss, J., Forstmann, B., Cramon, D.Y.v., 2005a. The role of the inferior frontal junction area in cognitive control. Trends Cogn. Sci. 9, 314–316.

Brass, M., Ullsperger, M., Knoesche, T.R., Cramon, D.Y.v., Phillips, N.A., 2005b. Who comes first? The role of the prefrontal and parietal cortex in cognitive control. J. Cognit. Neurosci. 17, 1367–1375.

Britz, J., Landis, T., Michel, C.M., 2009. Right parietal brain activity precedes perceptual alternation of bistable stimuli. Cereb. Cortex 19, 55–65.

Busch, N.A., Dubois, J., VanRullen, R., 2009. The phase of ongoing EEG oscillations predicts visual perception. J. Neurosci. 29, 7869–7876.

Carter, C.S., Braver, T.S., Barch, D.M., Botvinick, M.M., Noll, D., Cohen, J.D., 1998. Anterior cingulate cortex, error detection, and the online monitoring of performance. Science 280, 747–749.

Carter, C.S., van Veen, V., 2007. Anterior cingulate cortex and conflict detection: an update of theory and data. Cognitive, Affective, & Behavioral Neuroscience 7, 367–379.

Cavanagh, J.F., Cohen, M.X., Allen, J.J.B., 2009. Prelude to and resolution of an error: EEG phase synchrony reveals cognitive control dynamics during action monitoring. J. Neurosci. 29, 98–105.

Corbetta, M., 1998. Frontoparietal cortical networks for directing attention and the eye to visual locations: Identical, independent, or overlapping neural systems? Proc. Natl. Acad. Sci. U.S.A. 95, 831–838.

Corbetta, M., Patel, G., Shulman, G.L., 2008. The reorienting system of the human brain: from environment to theory of mind. Neuron 58, 306–324.

Debener, S., Ullsperger, M., Siegel, M., Fiehler, K., von Cramon, D.Y., Engel, A.K., 2005. Trial-by-trial coupling of concurrent electroencephalogram and functional magnetic resonance imaging identifies the dynamics of performance monitoring. J. Neurosci. 25, 11730–11737.

Ducommun, C.Y., Murray, M.M., Thut, G., Bellmann, A., Viaud-Delmon, I., Clarke, S., Michel, C.M., 2002. Segregated processing of auditory motion and auditory location: an ERP mapping study. Neuroimage 16, 76–88.

Fuchs, M., Wagner, M., Köhler, T., Wischmann, H.-A., 1999. Linear and nonlinear current density reconstructions. J. Clin. Neurophysiol. 16, 267–295.

Gonzalez Andino, S.L., Michel, C.M., Thut, G., Landis, T., Grave de Peralta, R., 2005. Prediction of response speed by anticipatory high-frequency (gamma band) oscillations in the human brain. Hum. Brain Mapp. 24, 50–58.

Groening, K., Brodbeck, V., Moeller, F., Wolff, S., van Baalen, A., Michel, C.M., Jansen, O., Boor, R., Wiegand, G., Stephani, U., Siniatchkin, M., 2009. Combination of EEG-fMRI and EEG source analysis improves interpretation of spike-associated activation networks in paediatric pharmacoresistant focal epilepsies. Neuroimage 46, 827–833.

Hajcak, G., Nieuwenhuis, S., Ridderinkhof, K.R., Simons, R.F., 2005. Error-preceding brain activity: robustness, temporal dynamics, and boundary conditions. Biol. Psychol. 70, 67–78.

Hanslmayr, S., Aslan, A., Staudigl, T., Klimesch, W., Herrmann, C.S., Bäuml, K.-H., 2007. Prestimulus oscillations predict visual perception performance between and within subjects. Neuroimage 37, 1465–1473.

Hanslmayr, S., Klimesch, W., Sauseng, P., Gruber, W., Doppelmayr, M., Freunberger, R., Pecherstorfer, T., 2005. Visual discrimination performance is related to decreased alpha amplitude but increased phase locking. Neurosci. Lett. 375, 64–68.

Herrmann, M.J., Rommler, J., Ehlis, A.-C., Heidrich, A., Fallgatter, A.J., 2004. Source localization (LORETA) of the error-related-negativity (ERN/Ne) and positivity (Pe). Cogn. Brain Res. 20, 294–299.

Kondakor, I., Lehmann, D., Michel, C.M., Brandeis, D., Kochi, K., Koenig, T., 1997. Prestimulus EEG microstates influence visual event-related potential microstates in field maps with 47 channels. J. Neural Transm. V104, 161–173.

Kondakor, I., Pascual-Marqui, R.D., Michel, C.M., Lehmann, D., 1995. Event-related potential map differences depend on the prestimulus microstates. J. Med. Eng. Technol. 19, 66–69.

Kranczioch, C., Debener, S., Maye, A., Engel, A.K., 2007. Temporal dynamics of access to consciousness in the attentional blink. Neuroimage 37, 947–955.

Krzanowski, W., Lai, Y.T., 1988. A criterion for determining the number of groups in a data set using sum of squares clustering. Biometrics 44, 23–34.

Lantz, G., Holub, M., Ryding, E., Rosen, I., 1996. Simultaneous intracranial and extracranial recording of interictal epileptiform activity in patients with drug resistant partial epilepsy: patterns of conduction and results from dipole reconstructions. Electroencephalogr. Clin. Neurophysiol. 99, 69–78.

Lehmann, D., Michel, C.M., Pal, I., Pascual-Marqui, R.D., 1994. Event-related potential maps depend on prestimulus brain electric microstate map. Int. J. Neurosci. 74, 239–248.

Luu, P., Tucker, D.M., Makeig, S., 2004. Frontal midline theta and the error-related negativity: neurophysiological mechanisms of action regulation. Clin. Neurophysiol. 115, 1821–1835.

MacLeod, C.M., 1991. Half a century of research on the Stroop effect: an integrative review. Psychol. Bull. 109, 163–203.

Michel, C.M., de Peralta, R.G., Lantz, G., Andino, S.G., Spinelli, L., Blanke, O., Landis, T., Seeck, M., 1999a. Spatiotemporal EEG analysis and distributed source estimation in presurgical epilepsy evaluation. J. Clin. Neurophysiol. 16, 239–266.

Michel, C.M., Murray, M.M., Lantz, G., Gonzalez, S., Spinelli, L., Grave de Peralta, R., 2004. EEG source imaging. Clin. Neurophysiol. 115, 2195–2222.

Michel, C.M., Seeck, M., Landis, T., 1999b. Spatiotemporal dynamics of human cognition. News Physiol. Sci. 14, 206–214.

Michel, C.M., Thut, G., Morand, S., Khateb, A., Pegna, A.J., Grave de Peralta, R., Gonzalez, S., Seeck, M., Landis, T., 2001. Electric source imaging of human brain functions. Brain Res. Rev. 36, 108–118.

Mohr, C., Michel, C.M., Lantz, G., Ortigue, S., Viaud-Delmon, I., Landis, T., 2005. Brain state-dependent functional hemispheric specialization in men but not in women. Cereb. Cortex 15, 1451–1458.

Murray, M., Brunet, D., Michel, C., 2008. Topographic ERP analyses: a step-by-step tutorial review. Brain Topogr. 20, 249–264.

Oldfield, R.C., 1971. The assessment and analysis of handedness: the Edinburgh inventory. Neuropsychologia 9, 97–113.

Pascual-Marqui, R.D., Michel, C.M., Lehmann, D., 1994. Low resolution electromagnetic tomography: a new method for localizing electrical activity in the brain. Int. J. Psychophysiol. 18, 49–65.

Perrin, F., Pernier, J., Bertrand, O., Echallier, J.F., 1989. Spherical splines for scalp potential and current density mapping. Electroencephalogr. Clin. Neurophysiol. 72, 184–187.

Ridderinkhof, K.R., Nieuwenhuis, S., Bashore, T.R., 2003. Errors are foreshadowed in brain potentials associated with action monitoring in cingulate cortex in humans. Neurosci. Lett. 348, 1–4.

Rihs, T.A., Michel, C.M., Thut, G., 2007. Mechanisms of selective inhibition in visual spatial attention are indexed by α-band EEG synchronization. Eur. J. Neurosci. 25, 603–610.

Rihs, T.A., Michel, C.M., Thut, G., 2009. A bias for posterior [alpha]-band power suppression versus enhancement during shifting versus maintenance of spatial attention. Neuroimage 44, 190–199.

Romei, V., Brodbeck, V., Michel, C., Amedi, A., Pascual-Leone, A., Thut, G., 2008a. Spontaneous fluctuations in posterior {alpha}-band EEG activity reflect variability in excitability of human visual areas. Cereb. Cortex 18, 2010–2018.

Romei, V., Rihs, T., Brodbeck, V., Thut, G., 2008b. Resting electroencephalogram alpha-power over posterior sites indexes baseline visual cortex excitability. Neuroreport 19, 203–208 210.1097/WNR.1090b1013e3282f1454c1094..

Rorden, C., Brett, M., 2000. Stereotaxic display of brain lesions. Behavioural Neurology 12, 191–200.

Schulz, E., Maurer, U., van der Mark, S., Bucher, K., Brem, S., Martin, E., Brandeis, D., 2008. Impaired semantic processing during sentence reading in children with dyslexia: combined fMRI and ERP evidence. Neuroimage 41, 153–168.

Sperli, F., Spinelli, L., Seeck, M., Kurian, M., Michel, C.M., Lantz, G., 2006. EEG source imaging in pediatric epilepsy surgery: a new perspective in presurgical workup. Epilepsia 47, 981–990.

Spinelli, L., Gonzalez Andino, S., Lantz, G., Seeck, M., Michel, C.M., 2000. Electromagnetic inverse solutions in anatomically constrained spherical head models. Brain Topogr. 13, 115–125.

Thierry, G., Martin, C.D., Downing, P., Pegna, A.J., 2007. Controlling for interstimulus perceptual variance abolishes N170 face selectivity. Nat. Neurosci. 10, 505–511.

Thorpe, S.J., Fabre-Thorpe, M., 2001. NEUROSCIENCE: seeking categories in the brain. Science 291, 260–263.

Thut, G., Nietzel, A., Brandt, S.A., Pascual-Leone, A., 2006. {alpha}-Band electroencephalographic activity over occipital cortex indexes visuospatial attention bias and predicts visual target detection. J. Neurosci. 26, 9494–9502.

Tibshirani, R., Walther, G., 2005. Cluster validation by prediction strength. Journal of Computational & Graphical Statistics 14, 511–528.

Trujillo, L.T., Allen, J.J.B., 2007. Theta EEG dynamics of the error-related negativity. Clin. Neurophysiol. 118, 645–668.

Tzourio-Mazoyer, N., Landeau, B., Papathanassiou, D., Crivello, F., Etard, O., Delcroix, N., Mazoyer, B., Joliot, M., 2002. Automated anatomical labeling of activations in SPM using a macroscopic anatomical parcellation of the MNI MRI single-subject brain. Neuroimage 15, 273–289.

van Veen, V., Carter, C.S., 2002a. The anterior cingulate as a conflict monitor: fMRI and ERP studies. Physiol. Behav. 77, 477–482.

van Veen, V., Carter, C.S., 2002b. The timing of action-monitoring processes in the anterior cingulate cortex. J. Cognit. Neurosci. 14, 593–602.

Vulliemoz, S., Thornton, R., Rodionov, R., Carmichael, D.W., Guye, M., Lhatoo, S., McEvoy, A.W., Spinelli, L., Michel, C.M., Duncan, J.S., Lemieux, L., 2009. The spatio-temporal mapping of epileptic networks: combination of EEG-fMRI and EEG source imaging. Neuroimage 46, 834–843.

Weissman, D.H., Roberts, K.C., Visscher, K.M., Woldorff, M.G., 2006. The neural bases of momentary lapses in attention. Nat. Neurosci. 9, 971–978.

Womelsdorf, T., Fries, P., Mitra, P.P., Desimone, R., 2006. Gamma-band synchronization in visual cortex predicts speed of change detection. Nature 439, 733–736.

Zumsteg, D., Friedman, A., Wieser, H.G., Wennberg, R.A., 2006. Propagation of interictal discharges in temporal lobe epilepsy: correlation of spatiotemporal mapping with intracranial foramen ovale electrode recordings. Clin. Neurophysiol. 117, 2615–2626.